Biogeosciences, 9, 1–10, 2012
www.biogeosciences.net/9/1/2012/
doi:10.5194/bg-9-1-2012

Biogeosciences

An eddy-stimulated hotspot for fixed nitrogen-loss from the Peru oxygen minimum zone

M. A. Altabet[1], E. Ryabenko[2], L. Stramma[2], D. W. R. Wallace[3], M. Frank[2], P. Grasse[2], and G. Lavik[4]

[1]School for Marine Science and Technology, University of Massachusetts Dartmouth, 706 Rodney French Blvd, New Bedford, MA 02744-1221, USA
[2]GEOMAR Helmholtz Centre for Ocean Research Kiel, Düsternbrooker Weg 20, 24105 Kiel, Germany
[3]Halifax Marine Research Institute, Dalhousie University, 1355 Oxford Street, P.O. Box 15000, Halifax, Nova Scotia B3H 4R2, Canada
[4]Max Planck Institute for Marine Microbiology, Celsiusstr. 1, 28359 Bremen, Germany

Correspondence to: M. A. Altabet (maltabet@umassd.edu)

Received: 30 May 2012 – Published in Biogeosciences Discuss.: 2 July 2012
Revised: 25 October 2012 – Accepted: 1 November 2012 – Published:

Abstract. Fixed nitrogen (N) loss to biogenic N_2 in intense oceanic O_2 minimum zones (OMZs) accounts for a large fraction of the global N sink and is an essential control on the ocean's N-budget. However, major uncertainties exist regarding microbial pathways as well as net impact on the magnitude of N-loss and the ocean's overall N-budget. Here we report the discovery of a N-loss hotspot in the Peru OMZs associated with a coastally trapped mesoscale eddy that is marked by an extreme N-deficit matched by biogenic N_2 production, high NO_2^- levels, and the highest isotope enrichments observed so far in OMZs for the residual NO_3^-. High sea surface chlorophyll (SSC) in seaward flowing streamers provides evidence for offshore eddy transport of highly productive, inshore water. Resulting pulses in the downward flux of particles likely stimulated heterotrophic dissimilatory NO_3^- reduction and subsequent production of biogenic N_2 within the OMZs. A shallower biogenic N_2 maximum within the oxycline is likely a feature advected by the eddy streamer from the shelf. Eddy-associated temporal/spatial heterogeneity of N-loss, mediated by a local succession of microbial processes, may explain inconsistencies observed among prior studies. Similar transient enhancements of N-loss likely occur within all other major OMZs exerting a major influence on global ocean N and N isotope budgets.

1 Introduction

Extensive oxygen minimum zones (OMZs, also known as O_2 deficient zones – ODZ's) are found at intermediate depths in the Arabian Sea, off western Mexico, and off Peru and northern Chile. They arise regionally from poor ventilation of source waters and high downward fluxes of organic matter (OM) supporting subsurface respiration. In these regions, the lack of O_2 requires microbial heterotrophy to rely on oxidants other than O_2 and include those that result in the biogenic production of N_2 gas from chemically combined forms of N. These processes also occur in anoxic marine sediments and in sum, account for almost the entire N-loss from the oceans (Codispoti, 2007; Gruber, 2008) and thereby are essential terms in the ocean's N-budget. The balance with N-sources (from biologically mediated N_2 fixation, rivers and the atmosphere) controls the oceanic fixed-N inventory (primarily as NO_3^-) which, being an essential nutrient, is a major control on marine productivity. The overall magnitude of N-loss from OMZs is under debate and is a key determinant of whether the ocean's inventory of fixed-N is currently in steady-state or declining (Codispoti, 2007). Recent decadal-scale expansion of OMZs, a possible consequence of global warming (Stramma et al., 2008, 2009), suggests that oceanic N-loss could be increasing, underscoring the need to understand the present state of the ocean's N-budget and the processes that control it.

A number of interlinking microbial pathways contribute to N-loss in OMZs and control the corresponding production of biogenic N_2. Whereas heterotrophic denitrification (HDN; $NO_3^- \rightarrow N_2$ via NO_2^-) was canonically viewed as dominant, important roles are now ascribed to the chemosynthetic anammox process (ANM; $NO_2^- + NH_4^+ \rightarrow N_2$; Kuypers et al., 2003) as well as dissimilatory nitrate reduction to ammonia (DNRA; $NO_3^- \rightarrow NH_4^+$ via NO_2^-; Lam et al., 2009). Recent studies disagree as to whether HDN or ANM is the dominant process for producing biogenic N_2 (Ward et al., 2009; Bulow et al., 2010; Hamersley et al., 2007) and it remains unclear if these differences are the result of regional contrasts, time space^{-1} heterogeneity, or methodology (Voss and Montoya, 2009). Coupling these pathways can result in variable stoichiometry between NO_3^- removal and N_2 production provided there is an allochthonous supply of NH_4^+. However, recent comparison between NO_3^- deficits and biogenic N_2 in several OMZs are consistent with traditional stoichiometries (e.g. Chang et al., 2010), providing no evidence for allochthonous ammonium supporting the N-loss processes in the open ocean OMZs. These microbial processes do vary in their environmental sensitivities, such as threshold O_2 concentration (Kalvelage et al., 2011), so that knowledge of variability in their presence and activity is required for modeling and prediction of response to future global change.

Stable N isotope distributions in the ocean are also greatly influenced by N-loss processes (variations in $^{15}N/^{14}N$ are expressed in the $\delta^{15}N$ notation as ‰ difference from the ratio for atmospheric N_2). Dissimilatory NO_3^- reduction to NO_2^- is known to produce both strong N as well as O isotopic fractionation (Granger et al., 2008) leaving residual seawater NO_3^- enriched and the product NO_2^- depleted in ^{15}N and ^{18}O (Casciotti and McIlvin, 2007; fractionation factor, $\varepsilon \sim 25$ ‰). Presumably because ^{15}N-depleted N_2 gas is ultimately produced via preferential loss of ^{14}N, this process is responsible for enriching the oceanic fixed-N inventory in ^{15}N ($\delta^{15}N \sim 5$ ‰ relative to atmospheric N_2; Sigman et al., 2009) as compared to sources (e.g. -1 to -2 ‰ for N_2 fixation; Carpenter et al., 1997).

Regionally high $\delta^{15}N$ values for residual NO_3^- ($\delta^{15}NO_3^-$) in OMZs produce a corresponding signal in underlying sediments via upwelling and phytoplankton assimilation and downcore records reveal that OMZs N-loss has been highly sensitive to past climate change (e.g. Altabet et al., 2002). These isotopic effects have also been used to quantitatively constrain the modern ocean's N-budget. Due to physical transport limitation of substrates into and through sediments, benthic N-loss produces little isotopic fractionation as compared to water column N-loss in OMZs. This distinction allows isotopic mass balances and the average oceanic $\delta^{15}NO_3^-$ to be used to estimate the relative importance of N-loss in sediments vs. the water column, as well as the magnitude of the overall oceanic N sink (Brandes and Devol, 2002). However, such calculations are highly dependent on the choice of effective fractionation factors, which can be influenced by a number of environmental factors (Altabet, 2007) in addition to microbial pathways.

Whereas prior study of OMZs' N-loss processes have tacitly assumed a relatively stationary and homogeneous interior-ocean environment, the consequences of temporal/spatial variability, particularly with respect to episodic organic matter fluxes, have just begun to be recognized (Thamdrup et al. 2006; Ward et al., 2008, 2009; Dalsgaard et al., 2012). Assumed homogeneity was also once the case for studies of the near-surface ocean with respect to plankton productivity and community ecology. It is now well recognized that physical forcing of temporal spatial^{-1} heterogeneity not only produces physical patchiness but also results in higher average oceanic productivity (McGillicuddy and Robinson, 1997; McGillicuddy et al., 1998). This physical forcing and patchiness often occurs in the form and at the scale of mesoscale eddies. Here we show the first evidence for analogous interactions between eddies and OMZs' N-loss.

2 Sampling and analytical methods

The physical, chemical, and biological dynamics of the Peru OMZs were studied in a series of cruises carried out as part of the German-led Climate – Biogeochemistry Interactions in the Tropical Ocean program (www.sfb754.de) of the German Research Foundation. In January and February of 2009, a total of 121 stations were occupied between 1° N and 18° S and from the coast out to 85°50′ W, providing detailed spatial coverage of biogeochemical properties relevant to N-loss processes (Fig. 1a). At each station, water samples were collected using 12 l Niskin bottles on a CTD rosette system equipped with temperature, pressure, conductivity and oxygen sensors. Nutrients and oxygen were determined according to Grasshoff et al. (1999).

The isotopic composition of dissolved NO_3^- was measured using Cd-reduction to NO_2^- followed by reaction with azide to produce N_2O (McIlvin and Altabet, 2005). NaCl was added to ensure consistent quantitative yield (Ryabenko et al., 2009). Pre-existing NO_2^- was removed at the time of collection by addition of sulfanilic acid (Ryabenko et al., 2012). For NO_2^- isotopic analysis, a separate sample set was collected and preserved frozen and only the azide treatment was applied. International references USGS 34, USGS 35, and IAEA 3 were used for calibration. Samples were analyzed in both Germany (GEOMAR) and in the USA (SMAST) using a purge-trap isotope ratio mass spectrometer (PT-IRMS) system. Reproducibility was 0.3 and 0.6 ‰ for $\delta^{15}N$ and $\delta^{18}O$, respectively.

High precision N_2/Ar for detection of biogenic N_2 and δ^{15}N-N_2 were determined on septum sealed samples using on-line gas extraction system coupled to a multicollector IRMS (Bristow et al., 2012TS1). These data were produced by removing O_2 in the samples prior to introduction into the mass spectrometer to avoid artifacts associated with varying N_2/O_2 (Devol et al., 2006). In terms of calculated biogenic N_2, certainty is on the order of $\pm 1\,\mu mol\,kg^{-1}$. δ^{15}N-N_2 data were acquired during the same analytical sessions with a certainty of ± 0.05 ‰. Publicly available satellite data for sea surface chlorophyll (SSC) are from the NASA Giovanni website (http://gdata1.sci.gsfc.nasa.gov) and sea level anomaly (SLA) are from the AVISO website (http://www.aviso.oceanobs.com).

3 Results

3.1 Properties maps of Peru OMZs

For context, relevant biogeochemical properties are mapped along a constant density (isopycnal) surface to highlight the effects of non-conservative, N-cycling processes (Fig. 1). The chosen isopycnal density corresponding to $\sigma_\theta = 26.3\,kg\,m^{-3}$ varied between 100 and 170 m depth and was located vertically near the top of the minimum O_2 layer of the water column. South of 7 to 10° S, O_2 concentrations on this isopycnal surface were generally low enough to enable N-loss processes ($< 3\,\mu mol\,kg^{-1}$; Fig. 1a) consistent with prior observations (Codispoti and Christensen, 1985). Southward intensification of the OMZs along its northern boundary is associated with the poleward flow of the Peru Undercurrent (PUC) partly sourced in the lower equatorial undercurrent (Strub et al., 1987), comprising both the OMZs core and the primary source of upwelled waters in this region. Onset of dissimilatory NO_3^- reduction in the OMZs is marked by the pronounced appearance of NO_2^-, which is both an intermediate for HDN and DNRA, as well as a substrate for ANM (Fig. 1b). For most of the open ocean portion of the Peru OMZs, maximal $[NO_2^-]$ is $< 5\,\mu mol\,kg^{-1}$. Net N-loss as a consequence of NO_3^- conversion to N_2 gas has been previously estimated using N-deficit calculations based on anomalies in the oxidized forms of N relative to the Redfield proportionality with PO_4^{-3} (Devol et al., 2006):

$$N' = NO_3^- + NO_2^- - 16 \times PO_4^{-3} \quad (1)$$

The N-deficit, N′, is similar to the N* formulation (Gruber and Sarmiento, 1997) but without the latter's constant offset (Appendix A). NH_4^+ is not included as its concentration has been observed to be very low to non-detectable throughout much of our study area, particularly seaward of the shelf. South of 7 to 10° S, N′ decreases from −5 to −30 µmol/kg along $\sigma_\theta = 26.3\,kg\,m^{-3}$ confirming substantial N-loss correlated with the O_2 and NO_2^- observations (Fig. 1c). Consistent with N-loss via dissimilatory NO_3^- reduction, δ^{15}N values for residual NO_3^- are inversely correlated with N′ (Fig. 1d).

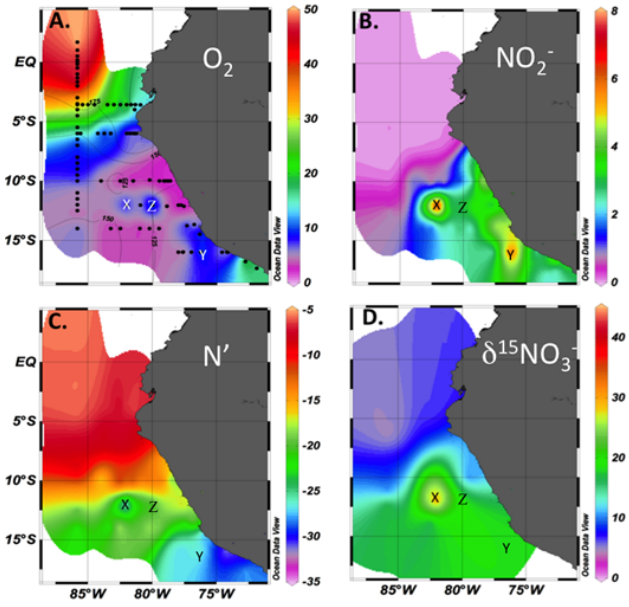

Fig. 1. Biogeochemical maps of the Peru OMZs from a series of stations constituting 6 transects normal and 1 transect parallel to the coast occupied during cruises M77/3 and M77/4 of the German research vessel R/V *Meteor* in January and February of 2009. Properties are shown along a constant density surface ($\sigma_\theta = 26.3\,kg\,m^{-3}$) within the upper portion of the OMZs corresponding to a depth range of 100 to 170 m. **(A)** O_2 concentration ($\mu mol\,kg^{-1}$), station locations, and density of $\sigma_\theta = 26.3\,kg\,m^{-3}$). **(B)** NO_{2-} concentration ($\mu mol\,kg^{-1}$). **(C)** Nitrogen anomaly $-N'$ ($\mu mol\,kg^{-1}$) calculated as $[NO_{3-}] + [NO_{2-}] - 16 \times [PO_4^{-3}]$. **(D)** The δ^{15}N of NO_{3-}. When southward intensification of suboxic conditions reaches $[O_2] < 5\,\mu mol\,kg^{-1}$, the onset of N-loss processes is evident. Location of Station 7, a hotspot for N-loss, is marked by an "X". Data smoothing to produce this visualization diminishes somewhat the extrema found at Station 7 (see Fig. 2). A second hotspot (Station 29) was also detected (marked by a "Y"), but is not discussed in the text due to a less comprehensive data set for this site. The position of a more normal comparison station (see Fig. 2) is marked by a "Z".

3.2 An N-loss hotspot

Our biogeochemical maps reveal one highly anomalous offshore station (12° S 82° W, Station 7) characterized by extreme values for N-loss indicators with respect to the background geographic gradients. We believe a 2nd hotspot is evident in these maps (Station 29, 16° S 76°27′ W) but is not discussed further due to a less comprehensive dataset available for this site. Station 7 is marked by strongly elevated $[NO_2^-]$ of up to $10\,\mu mol\,kg^{-1}$, high $\delta^{15}NO_3^-$, as well as very negative N′ signature (Fig. 2a) in comparison with surrounding stations including adjacent shoreward Station 9 (Figs. 1

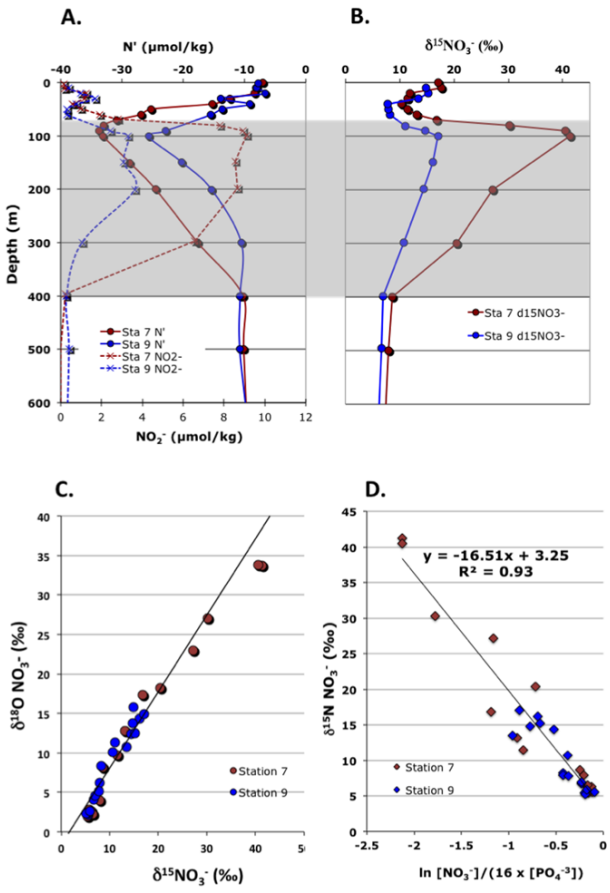

Fig. 2. Depth profiles for N-loss indicators at Station 7 showing extreme values as compared to nearby, shoreward Station 9. OMZs ($O_2 < 5\,\mu mol\,kg^{-1}$) indicated as a shaded depth interval (see also Fig. 3). **(A)** NO_2^- and N-deficit (N') concentration profiles ($\mu mol\,kg^{-1}$). **(B)** Profiles for $\delta^{15}NO_3^-$ (‰ relative atmospheric N_2). **(C)** Crossplot of the $\delta^{18}O$ vs. the $\delta^{15}N$ of NO_3^-. **(D)** Rayleigh plot of $\delta^{15}NO_3^-$ vs. the ln of the residual NO_3^- fraction assuming the NO_3 concentration prior to removal is approximated as $16\times[PO_4^{-3}]$. The inverse slope estimates the fractionation effect (ε) at ~17 ‰.

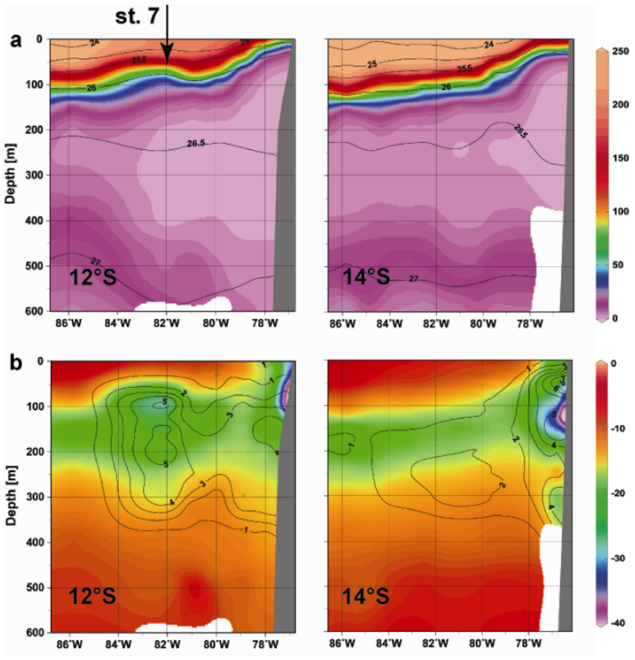

Fig. 3. Property distribution section off the Peru coast. **(A)** O_2 concentration ($\mu mol\,kg^{-1}$; color shading) and σ_θ (contour lines) sections at 12 and 14° S latitude (see station positions in Fig. 1). Station 7 is part of the 12° S section and its position is marked. **(B)** Corresponding N' (color shading) and NO_2^- concentration (contour lines) sections at 12 and 14° S. Units are in $\mu mol\,kg^{-1}$. Data smoothing to produce this visualization diminishes somewhat the extrema found at Station 7 (see Fig. 2).

and 2). The highest measured values of $\delta^{15}N$ and $\delta^{18}O$ for OMZs NO_3^- that we are aware of, are also observed at this station reaching 40 and 34 ‰ (Fig. 2b). In contrast, ocean-wide $\delta^{15}NO_3^-$ averages are near 5 and 2 ‰, respectively (Sigman et al., 2009). At our other Peru OMZs stations, maximal $\delta^{15}NO_3^-$ is typically ~15 ‰ and values as high as 24 ‰ have been reported from other OMZs (Altabet et al., 1999). Although the extrema are relatively shallow (100 m), these N-loss indicators at Station 7 extend broadly over the water column down to 400 m depth, corresponding to the layer of lowest O_2 concentration (Figs. 2, 3). Sections for N' and $[NO_2^-]$ on a E–W transect at 12° S also confirm Station 7 to be distinct as compared to neighboring stations, particularly with respect to the greater vertical extent of maxima. In contrast, the adjacent section at 14° S shows no evidence for an offshore N-loss hotspot (Fig. 3).

Dissimilatory NO_3^- reduction to NO_2^- is known to produce N and O isotopic fractionation with a characteristic slope near 1 (Granger et al., 2008). Deviations from this relationship are a common feature of the limited data sets available for OMZs and have been interpreted as evidence for co-occurrence of other N-transformation processes including NO_2^- oxidation and contributions from N_2 fixation (Casciotti and McIlvin, 2007; Sigman et al., 2005). In contrast, at Station 7 as well as nearby stations with less extreme N-loss indicators (e.g. Station 9), co-variation between NO_3^- $\delta^{15}N$ and $\delta^{18}O$ is indistinguishable from a slope of 1, implying dominance of NO_3^- reduction both at this site and more regionally (Fig. 2c). A Rayleigh fractionation model (Fig. 2d) can be used to estimate an "apparent" fractionation factor (ε) for N-loss assuming approximation to a closed system as done in prior studies (e.g. Voss et al., 2001). ε is found to be lower (~17 ‰; Fig. 2d) than previously considered typical for OMZs N-loss for both Stations 7 and 9, consistent with this being typical of the average behavior for the Peru OMZs (Ryabenko et al., 2012), given this method of data treatment.

3.3 Biogenic N_2

The amount of biogenic N_2 production resulting from N-loss processes (HDN or ANM) can be estimated from high precision N_2/Ar determinations (Chang et al., 2010). Biogenic N_2 production increases the measured N_2/Ar ratio over the value predicted from equilibration with the atmosphere at in situ temperature and salinity. Deviations from equilibrium N_2/Ar ratios are also known to arise from physical processes such as bubble injection in water mass formation regions. Our data are adjusted as previously described to account for this (Chang et al., 2010), allowing estimation of an "excess" N_2 concentration due to biological processes. Biogenic N_2 concentrations below the oceanic mixed layer can also be predicted using Richards stoichiometry (Richards, 1965) which takes into account nitrogen originating from the breakdown of OM that does not appear as NH_4^+ and is assumed to be also converted to N_2 (Appendix A):

$$N_{2\ \text{biogenic}}\left(\text{as } \mu\text{mol kg}^{-1}\,N_2\right) = \left(N'_{\text{source waters}} - N'_{\text{OMZs}}\right) \times 0.5 \quad (2)$$

Measured biogenic N_2 concentrations throughout the OMZs at Station 7 (70 to 400 m) closely follows concentrations predicted from the N′ data (Fig. 4a) suggesting that NO_3^- removal is well balanced by biogenic N_2 production even for these relatively high OMZs values. However, measured biogenic N_2 concentrations in the oxycline of Station 7, above the core of the OMZs (50 to 70 m), are twice as high as the values predicted from N′ and >20 times our analytical uncertainty. Our observations at other "normal" offshore stations, as well as recently published data (Chang et al., 2010), do not show this unusual feature.

The biogenic N_2 maximum at 50 to 70 m at Station 7 is also unique with respect to its isotopic composition. Our method for N_2/Ar determination allows the δ^{15}N of dissolved N_2 to be measured at very high precision (better than ± 0.05 ‰), which provides further information concerning the source of biogenic N_2. Such high precision is needed to detect the isotopic ratio of the biogenic N_2 above the large background of atmospheric N_2. We calculate predicted δ^{15}N N_2 anomalies relative to the atmospheric background based on an isotope mass balance with NO_3^- and NO_2^-. We assume that the mass-weighted difference between δ^{15}N of source and OMZs waters must be reflected in biogenic N_2 (Appendix A). As with biogenic N_2 concentration, the predicted anomalies in the δ^{15}N of total N_2 (atmospheric background plus biogenic) are in agreement with the measured values throughout most of the OMZs (Fig. 4b). Together these data are consistent with a simple mass balance between NO_3^- removal and biogenic N_2 production. However, large discrepancies between measured and predicted isotopic ratios are observed within the oxycline, where a 0.25 ‰ higher than expected signal is observed at the biogenic N_2 maximum (Fig. 4b). Whereas the predicted δ^{15}N of the biogenic N_2 component alone ranges from -5 to $+3$ ‰ (also from NO_3^- and NO_2^- isotope mass balance), these measurements imply that the δ^{15}N of the biogenic N_2 at this depth is substantially higher, $\sim +5$‰ . This implies that the allochthonous biogenic N_2 found in the oxycline was produced from NO_3^- (or NH_4^+) with little isotope fractionation and is distinct from the apparent autochthonous source within the OMZs below it.

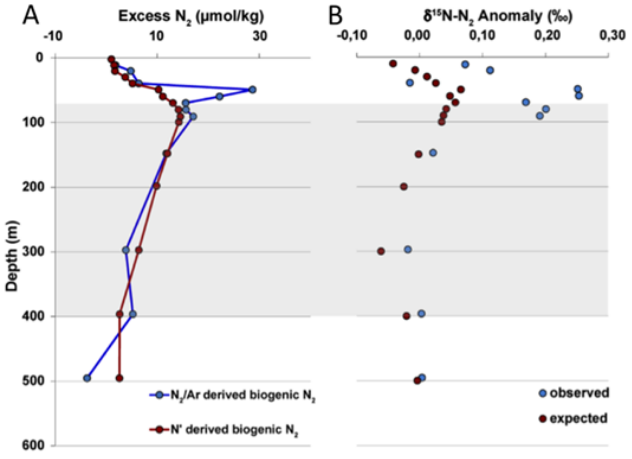

Fig. 4. Biogenic N_2 depth profiles at Station 7. **(A)** Measured and expected excess N_2 (biogenic) concentration (µmol kg^{-1}). **(B)** The measured and expected δ^{15}N anomaly for N_2. OMZs indicated as a shaded depth interval. Expected biogenic N_2 is derived from the nitrogen anomaly (N′) assuming Richards stoichiometry (Richards, 1965) after taking into account N′ for water masses upstream of the OMZs (Appendix A). Measured biogenic N_2 is calculated from deviations in N_2/Ar ratio from values expected at saturation with the atmosphere at in situ temperature and salinity and adjusted for physical sources of N_2/Ar anomaly by comparison with stations outside the OMZs (Chang et al., 2010). The expected δ^{15}N anomaly for N_2 is based on isotopic mass balance between the system's source NO_3^- and OMZs NO_3^- and NO_2^- (Appendix A).

Two separate sets of phenomena thus appear to have contributed to the N-loss hotspot at Station 7. Our biogeochemical and isotopic indicators support the formation of the relatively large amounts of biogenic N_2 within in the OMZs at Station 7 through canonical processes (reduction of pre-existing NO_3^-). However, the biogenic N_2 observed within the oxycline appears to have formed rather differently since it (1) is present in oxygenated waters, (2) is found at levels stoichiometrically inconsistent with observed N′ and (3) has an isotopic composition that is also inconsistent with production from pre-exiting NO_3^-. We will discuss below a likely shelf source for this biogenic N_2 found above the OMZs.

3.4 Eddy impacts

Previously, patches of high [NO_2^-] along the Peru margin were found to be associated with seaward current jets (Friederich and Codispoti, 1987). Understanding the N-loss hotspot status of Station 7 therefore likely requires consid-

eration of any synoptic mesoscale variability. As observed from satellite images, both anticyclonic and cyclonic eddies are important and persistent features of the circulation of this coastal upwelling system, as well as of the eastern tropical South Pacific as a whole (Chaigneau et al., 2008). Off Peru, coherent eddies are typically formed along the coast and propagate westward at 3 to 6 km d^{-1} and have a mean eddy lifetime of $\sim$1 month. Their mean radius is 80 km, increasing equatorward due to the increasing Rossby Radius of Deformation. Eddies are most frequently observed off Chimbote (9° S) and south of San Juan (15° S), north and south of Station 7. As detected by satellite sea surface chlorophyll (SSC; phytoplankton concentration) and satellite sea level anomaly (SLA; mesoscale circulation), Station 7 was located on the seaward flank of a large eddy trapped near the coast and centered near 11° S and 80.5° W (Fig. 5). Further evidence of Station 7's having been located within the edge of an anticyclonic eddy is seen in the O_2 section at 12° S, which shows this station to be located at the periphery of a "bowl-like" distribution (Fig. 3). The region inshore of Station 7 with deepening oxycline on this section includes Station 9 and corresponds to part of the eddy's interior. Note that Station 7 was occupied on 5 January 2009, whereas the SSC map is an average for the entire month. However, the SLA data represent a 1-day snapshot for 7 January 2009 and the overlay between the current vectors and SSC suggest that the eddy was relatively stationary in this location throughout the observation period. In fact, SSC images for December 2008 and February 2009 also show the eddy to be in the same location.

The SSC imagery reveals low phytoplankton concentrations at the eddy's center and high values around most of its periphery. To the northwest, a high SSC filament appears to have been pulled offshore from the highly productive inshore upwelling region perhaps through interaction between the eddy's circulation and the equatorward mean flow at the surface in this region. Very high inshore productivity is associated with intense upwelling of nutrient-rich (NO_3^-, PO_4^{-3}, and silicate) waters on the shallow shelf, coupled with Fe release from the sediment that relieves Fe limitation (Bruland et al., 2005). SLA reflects current structures superimposed on the mean flow. When overlaid on the SSC map, current vectors derived from the satellite SLA data confirm the eddy to be a strong anticyclonic feature as well as the offshore motion of the northwestern SSC filament (Fig. 5). Given the observed eddy size and an estimated swirl velocity of $\sim$20 km d^{-1} estimated from the SLA data and on board ADCP measurements, it took approximately 20 days to transport coastal water to the location of Station 7. Thus there is sufficient time for this and other eddies to impact offshore waters as also shown by the observed offshore flowing SSC filament.

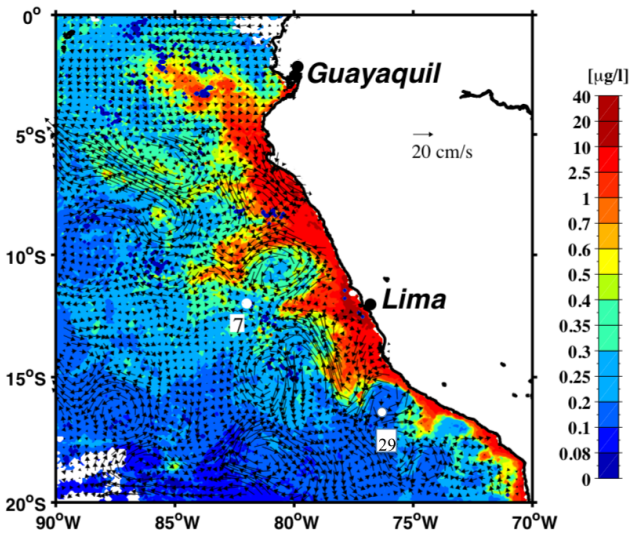

Fig. 5. Satellite observations for the period when Station 7 was occupied (location as indicated). Sea surface chlorophyll (SSC; µg l^{-1}) for January 2009 is overlaid by current vectors derived from sea level anomaly (SLA) for 7 January 2009. SSC reflects surface ocean phytoplankton concentration and productivity and was available from the NASA Giovanni website (http://gdata1.sci.gsfc.nasa.gov) as a monthly average. SLA and related current vectors vary in response to barotropic velocity variation from the mean state and is available from the AVISO website (http://www.aviso.oceanobs.com) representing the sea state for a given day.

4 Discussion

We have identified a "hotspot" for N-loss in the Peru OMZs based on the distribution of N′, NO_2^-, and $\delta^{15}NO_3^-$. However, two separate sets of phenomena appear responsible for the biogenic N_2 accumulated within and above the OMZs. Due to volumetric considerations, the biogenic N_2 within the OMZs (70 to 400 m) is the predominant contributor to the total at Station 7 and its N-loss hotspot status. Mass balance considerations and isotope analysis furthermore supports its formation by in situ stimulation of the conversion of NO_3^- to N_2 in the OMZs through a combination of HDN, DNRA, and/or ANM without extraneous NH_4^+ sources for the latter. This stimulation, in turn, appears to be the result of Station 7's being located near or within the seaward edge of a coastally trapped, anticyclonic eddy (Fig. 5). A particular role for eddies in producing N-loss hotspots in association with seaward flowing streamers can account for the uniqueness of this observation (aside from possibly Station 29) as the station grid (Fig. 1) was not designed to resolve synoptic eddy features. It was happenstance that Station 7 was positioned at the seaward flank of a large coastal eddy.

The eddy likely produced the within-OMZs N-loss hotspot through offshore transport of highly productive inshore waters in the form of a high SSC streamer in its northwestern quadrant. We hypothesize that the subsequent down-

ward pulse of OM in the form of sinking particles stimulates localized N-loss, given the heterotrophic nature of HDN and DNRA processes (Bulow et al., 2010; Thamdrup et al., 2006). While ANM is autotrophic, it is also dependent on NH_4^+ and NO_2^- supplied by heterotrophic denitrification, DNRA, or other NO_3^- reducers. Thus dissimilatory NO_3^- reduction and concomitant production of biogenic N_2 is likely controlled by the OM flux (Ward et al., 2008) which, if episodic, would produce subsurface N-loss hotspots. Although high SSC was not found directly at Station 7, a modest temporal spatial^{-1} displacement would be expected between near-surface phytoplankton blooms, bloom collapse, the subsequent downward organic flux, and the appearance of N-loss indicators.

The maxima in biogenic N_2 found within the oxycline is, in contrast, likely an advected feature not produced by locally stimulated N-loss in deep offshore waters. Shelf water was clearly advected offshore in the eddy streamer (Fig. 5), suggesting that the biogenic N_2 unexpectedly found within the oxycline at 50 to 70 m had been exported from the inner shelf. These depths are shallow enough for these layers to have been in contact with shelf sediments, a likely direct or indirect source of biogenic N_2. By contrast, the larger quantity of biogenic N_2 found within the OMZs at Station 7 is too deep to have been advected from the shelf since most of the corresponding isopycnal surfaces intersect the upper slope (Figs. 2, 3). Given that the shallow biogenic N_2 peak is almost 3 times higher than expected from coincident N′, it is best explained by either biogenic N_2 production in shelf sediments and/or NH_4^+ release from sediments that is subsequently consumed by ANM in the water column. As such, this high biogenic N_2 feature is in itself evidence of direct eddy streamer influence at Station 7 despite a lack of locally high SSC. The high δ^{15}N value for the biogenic N_2 maximum is also consistent with a sediment source, where complete removal of fixed-N produces N_2 with little or no isotope fractionation (Brandes and Devol, 1997).

An implication of our observations is that coastally trapped eddies can increase the magnitude of regional N-losses through enhanced OM transport to the deep OMZs. Offshore transport of highly productive inshore waters inject large pulses of OM into the deep OMZs that would otherwise be respired in near surface oxygenated waters or sequestered by inner shelf sediments. By providing fuel for deep-ocean microbial N-loss processes, eddies thereby enhance the OMZs overall N-loss relative to OM production. Assuming conventional Redfield (1958) and Richards (1965) stoichiometry, photoautotrophic conversion of 30 µmol kg^{-1} of NO_3^- in the upper 30 m of upwelled water would produce enough OM to deplete 20 µmol kg^{-1} of NO_3^- from the upper 250 m of the offshore OMZs. Eddy lifetime and swirl velocity appear sufficient for this OM to be both produced within the streamers and to sink into the OMZs. When added to the "background" NO_3^- removal observed throughout the Peru OMZs (Fig. 1), the extreme magnitudes of the N-loss indicators observed at Station 7 are readily explained.

A second implication is that coastal eddies create previously unrecognized spatial as well as temporal variability in deep OMZs biogeochemistry. Hence, apparently inconsistent results among prior studies with respect to the rates of dominant pathways (Thamdrup et al., 2006; Ward et al., 2009; Bulow et al., 2010; Hamersley et al., 2007; Lam et al., 2009) may be explained by station positions that varied relative to the eddy field. Pulses of OM from eddy streamers would also produce temporal succession in the underlying OMZs microbial community. In the oxycline and above, remineralization of OM, production of NH_4^+, and nitrification (and perhaps N_2O production) would be transiently enhanced as suggested by earlier observations (Friederich and Codispoti, 1987). Subsequent sinking of OM into the OMZs would stimulate heterotrophic processes supported by NO_3^- reduction, leading to the observed accumulation of NO_2^- and N deficits. Pulses of HDN ("stop and go denitrification") may also lead to N_2O production (an intermediate in the biochemistry for HDN; Naqvi et al., 2000). NH_4^+ produced directly from OM and/or DNRA would in turn stimulate ANM. A similar microbial succession in response to OM pulses was also called upon by Dalsgaard et al. (2012) to explain relatively constant rates of ANM but sporadic higher rates of HDN in the Peru – N. Chile OMZs. Overall, the Peru OMZs should be viewed as a dynamic system impacted by episodic physical forcing of OM flux that increases N-loss via microbial transformations to biogenic N_2. This perspective is critical for the design of future field programs.

Finally, the observed extreme enrichments of NO_3^- ^{15}N and ^{18}O imply that important revisions to global ocean fixed-N and N isotope budgets may be required. Because sedimentary denitrification produces little N-isotopic fractionation (Brandes and Devol, 1997), the ratio of the average ^{15}N enrichment in the whole ocean ($\sim$ 7 ‰ compared to sources) to the OMZs denitrification effect ($\sim$ 25 ‰) has been used to estimate the relative contribution of OMZs to sedimentary N-loss (Brandes and Devol, 2002). It has been suggested however, that the effective OMZs fractionation effect has been overestimated and consequently its proportion of global marine N-loss has been underestimated (Altabet, 2007). Since the global rate of N-loss in OMZs is considered to be better constrained than for N-loss in sediments, too high a fractionation factor would also lead to overestimation of total oceanic N-loss and a budget that would imply that N sinks exceed sources. Here we show an apparent fractionation factor for N-loss lower than canonical for OMZs (17 vs. 25 ‰). Further, the extreme NO_3^- drawdown observed has important implications for the δ^{15}N of biogenic N_2, the term that directly impacts overall the N isotope budget. Extreme NO_3^- removal produces the extreme $\delta^{15}NO_3^-$ observed at Station 7 and requires, by mass balance, a less isotopically depleted biogenic N_2 product. Indeed, the calculated depth integrated

average δ^{15}N for biogenic N_2 within the OMZs at Station 7 is ~ -1 ‰ and thus only 6 ‰ less than the oceanic average $\delta^{15}NO_3^-$. When applied to global N isotope budgets, the resulting lower effective fractionation effect for OMZs N-loss also implies that OMZs account for a larger portion of overall oceanic N-loss than previously thought (Altabet, 2007) as well as an oceanic fixed-N budget closer to balance.

The impact of coastal mesoscale eddies on OMZs N-loss processes reported here is unlikely to be restricted to the waters off Peru, especially as the number of eddies can be greater in the other large OMZs, off Mexico and in the Arabian Sea (Chelton et al., 2011). However, OMZs also extend geographically far beyond the region of direct influence of coastal eddies, especially the one off Mexico (Codispoti and Richards, 1976). In oligotrophic open ocean regions, mesoscale eddies in particular are recognized as enhancing the vertical flux of nutrients and primary productivity (McGillicuddy and Robinson, 1997; McGillicuddy et al., 1998). Since most mesoscale eddies have recently been characterized as "non-linear" and capable of advecting water parcels, they have even greater potential for biogeochemical impact on the subsurface ocean (Chelton et al., 2011). Open-ocean eddies may thus produce similar "hotspots" for microbially mediated N-loss even in portions of OMZs that are distant from productive coastal waters.

Appendix A

A1 Use of N′ to estimate NO_3^- removal and production of biogenic N

Outside of OMZs, NO_3^- generally varies in stoichiometric proportion with PO_4^{-3} and O_2 as originally observed by Redfield (Redfield, 1958). Negative deviations in $[NO_3^-]$ from values expected from these proportions has been termed the NO_3^- deficit and is used to estimate net removal and production of biogenic N_2 in OMZs (Devol et al., 2006). The commonly used N* ($= [NO_3^-] - 16 \times [PO_4^{-3}] + 2.9$; Gruber and Sarmiento, 1997) assumes NO_3^- as the only form of dissolved inorganic N, uses the Redfield N : P ratio, and applies an offset of 2.9 that allows for global average N* to be 0. We have used a modification of N* ($N' = NO_3^- + NO_2^- - 16 \times PO_4^{-3}$), which takes into account NO_2^-, which can be found at significant concentrations in OMZs, and forgoes the global offset as not being relevant regionally. N′ slightly overestimates actual NO_3^- removal (a more negative N′) because of PO_4^{-3} release from organic matter breakdown by about 16 % (Devol et al., 2006). Accordingly, biogenic N_2 ($N_{2\ \mathrm{biogenic}}$) assuming equivalence with NO_3^- removal as well as Richards' stoichiometry (1.71 NO_3^- : 1 N_2; Richards, 1965) and taking into account conversion of organic N to N_2, can be calculated as:

$$N_{2\ \mathrm{biogenic}}\,(\text{as } \mu\mathrm{mol}N_2) = \left(N'_{\mathrm{source}} - N'_{\mathrm{OMZs}}\right) \times 0.86/1.71 \quad \text{(A1)}$$

$$N_{2\ \mathrm{biogenic}} \sim \left(N'_{\mathrm{source}} - N'_{\mathrm{OMZs}}\right) \times 0.5 \quad \text{(A2)}$$

Because the corrections for PO_4^{-3} production and N_2 produced from organic N-breakdown assume the same elemental stoichiometry for organic matter, they effectively cancel each other.

The N'_{source} term accounts for source waters not necessarily having zero N anomaly. It was measured at stations upstream from the OMZs on isopycnal surfaces corresponding to those bounding the Peru OMZs and is about -5 µmol kg^{-1} in this system. Figure 3a compares biogenic N_2 calculated in this fashion (N′ derived) with measured values (from N_2/Ar).

A2 Anomaly in the δ^{15}N of N_2

The δ^{15}N-N_2 anomaly reported is the difference between the measured value and the value expected at atmospheric equilibrium at in situ temperature and salinity (between 0.6 and 0.8 ‰). For the measured anomaly, the difference between measured δ^{15}N-N_2 and the equilibrium value is reported (Fig. 4b). For the expected anomaly, the δ^{15}N of biogenic N_2 is first calculated from isotope mass balance between source NO_3^- and OMZs NO_3^- and NO_2^- assuming differences are accounted for by production of biogenic N_2:

$$\delta^{15}\mathrm{N}{-}N_{2\ \mathrm{biogenic}} = \left(\delta^{15}\mathrm{N}{-}NO_{3\ \mathrm{source}}^- \times \left[NO_3^-\right]_{\mathrm{source}} - \left[NO_{3\mathrm{OMZs}}^-\right] \times \delta^{15}\mathrm{N}{-}NO_{3\ \mathrm{OMZs}}{}^- - \left[NO_2^-\right]_{\mathrm{OMZs}} \times \delta^{15}\mathrm{N}{-}NO_{2\ \mathrm{OMZs}}^-\right) / \left[N_{2\ \mathrm{biogenic}}\right] \quad \text{(A3)}$$

$$\left[NO_3^-\right]_{\mathrm{source}} = 16 \times PO_{4\ \mathrm{OMZs}}^{-3} + N'_{\mathrm{source}} \quad \text{(A4)}$$

As for N'_{source}, δ^{15}N-$NO_{3\ \mathrm{source}}^-$ is measured at stations upstream of the Peru OMZs and is about 7 ‰. Not included is the isotopic signal from the small amount of biogenic N_2 produced from organic N, which would be expected to produce a modest increase in its δ^{15}N value in this system.

The expected δ^{15}N-N_2 anomaly is calculated by addition of the biogenic N_2 signal with the background N_2 of atmospheric origin ($N_{2\ \mathrm{atm}}$; calculated assuming equilibrium at in situ temperature and salinity) with zero δ^{15}N anomaly;

$$\delta^{15}\mathrm{N}{-}N_{2\ \mathrm{anomaly}} = \left(\left[N_{2\ \mathrm{atm}}\right] \times \delta^{15}\mathrm{N}{-}N_{2\ \mathrm{atm}} + \left[N_{2\ \mathrm{biogenic}}\right] \times \delta^{15}\mathrm{N}{-}N_{2\ \mathrm{biogenic}}\right) / \left(\left[N_{2\,\mathrm{atm}}\right] + \left[N_{2\ \mathrm{biogenic}}\right]\right) \quad \text{(A5)}$$

Acknowledgements. Enrique Montes aided in sample collection and Jen Larkum and Laura Bristow provided critical technical assistance. Funding to MAA was provided by the US National Science Foundation. Funding to ER, LS, DW, MF, PG and GL

was provided by the Deutsche Forschungsgemeinschaft-supported project SFB-754 (www.sfb754.de). The R/V *Meteor* M77/3 and M77/4 Pacific cruises were granted by the DFG and the crews and captain of R/V *Meteor* are thanked for their help during cruises M77/3 and M77/4.

Edited by: B. Dewitte

References

Altabet, M. A.: Constraints on oceanic N balance/imbalance from sedimentary ^{15}N records, Biogeosciences, 4, 75–86, doi:10.5194/bg-4-75-2007, 2007.

Altabet, M. A., Murray, D. W., and Prell, W. L.: Climatically linked oscillations in Arabian Sea denitrification over the past 1 m.y.: Implications for the marine N cycle, Paleoceanography, 14, 732–743, doi:10.1029/1999PA900035, 1999.

Altabet, M. A., Higginson, M. J., and Murray, D. W.: The effect of millennial-scale changes in Arabian Sea denitrification on atmospheric CO_2, Nature, 415, 159–162, doi:10.1038/415159a, 2002.

Brandes, J. A. and Devol, A. H.: Isotopic fractionation of oxygen and nitrogen in coastal marine sediments, Geochim. Cosmochim. Ac., 61, 1793–1801, doi:10.1016/S0016-7037(97)00041-0, 1997.

Brandes, J. A. and Devol, A. H.: A global marine-fixed nitrogen isotopic budget: Implications for Holocene nitrogen cycling, Global Biogeochem. Cy., 16, 1120–1134, doi:10.1029/2001GB001856, 2002.

Bruland, K. W., Rue, E. L., Smith, G. J., and DiTullio, G. R.: Iron, macronutrients and diatom blooms in the Peru upwelling regime: brown and blue waters of Peru, Mar. Chem., 93, 81–103, doi:10.1016/j.marchem.2004.06.011, 2005.

Bulow, S. E., Rich, J. J., Naik, H. S., Pratihary, A. K., and Ward, B. B.: Denitrification exceeds anammox as a nitrogen loss pathway in the Arabian Sea oxygen minimum zone, Deep-Sea Res. Pt. 1, 57, 384–393, doi:10.1016/j.dsr.2009.10.014, 2010.

Carpenter, E. J., Harvey, H. R., Fry, B., and Capone, D. G.: Biogeochemical tracers of the marine cyanobacterium *Trichodesmium*, Deep-Sea Res. Pt. 1, 44, 27–38, doi:10.1016/S0967-0637(96)00091-X, 1997.

Casciotti, K. L. and McIlvin, M. R.: Isotopic analyses of nitrate and nitrite from reference mixtures and application to Eastern Tropical North Pacific waters, Mar. Chem., 107, 184–201, doi:10.1016/j.marchem.2007.06.021, 2007.

Chaigneau, A., Gizolme, A., and Grados, C.: Mesoscale eddies off Peru in altimeter records: Identification algorithms and eddy spatio-temporal patterns, Prog. Oceanogr., 79, 106–119, doi:10.1016/j.pocean.2008.10.013, 2008.

Chang, B. X., Devol, A. H., and Emerson, S. R.: Denitrification and the nitrogen gas excess in the eastern tropical South Pacific oxygen deficient zone, Deep-Sea Res. Pt. 1, 57, 1092–1101, doi:10.1016/j.dsr.2010.05.009, 2010.

Chelton, D. B., Schlax, M. G., and Samelson, R. M.: Global observations of nonlinear mesoscale eddies, Prog. Oceanogr., 91, 167–216, doi:10.1016/j.pocean.2011.01.002, 2011.

Codispoti, L. A.: An oceanic fixed nitrogen sink exceeding 400 Tg Na^{-1} vs. the concept of homeostasis in the fixed-nitrogen inventory, Biogeosciences, 4, 233–253, doi:10.5194/bg-4-233-2007, 2007.

Codispoti, L. A. and Christensen, J. P.: Nitrification, denitrification and nitrous-oxide cycling in the eastern tropical South-Pacific Ocean, Mar. Chemi., 16, 277–300, doi:10.1016/0304-4203(85)90051-9, 1985.

Codispoti, L. A. and Richards, F. A.: An analysis of the horizontal regime of denitrification in the eastern tropical North Pacific, Limnol. Oceanogr., 21, 379–388, 1976.

Dalsgaard, T., Thamdrup, B., Farías, L., and Peter Revsbech, N.: Anammox and denitrification in the oxygen minimum zone of the eastern South Pacific, Limnol. Oceanogr., 57, 1331–1346, doi:10.4319/lo.2012.57.5.1331, 2012.

Devol, A. H., Uhlenhopp, A. G., Naqvi, S. W. A., Brandes, J. A., Jayakumar, D. A., Naik, H., Gaurin, S., Codispoti, L. A., and Yoshinari, T.: Denitrification rates and excess nitrogen gas concentrations in the Arabian Sea oxygen deficient zone, Deep-Sea Res. Pt. 1, 53, 1533–1547, doi:10.1016/j.dsr.2006.07.005, 2006.

Friederich, G. E. and Codispoti, L. A.: An analysis of continuous vertical nutrient profiles taken during a cold-anomaly off Peru, Deep-Sea Res. Pt. 1, 34, 1049–1065, doi:10.1016/0198-0149(87)90052-5, 1987.

Granger, J., Sigman, D. M., Lehmann, M. F., and Tortell, P. D.: Nitrogen and oxygen isotope fractionation during dissimilatory nitrate reduction by denitrifying bacteria, Limnol. Oceanogr., 53, 2533–2545, doi:10.4319/lo.2008.53.6.2533, 2008.

Grasshoff, K., Kremling, K., and Ehrhardt, M.: Methods of seawater analysis – third, completely revised and extended version, Seawater Analysis Wiley-VCH, 1999. TS2

Gruber, N.: The marine nitrogen cycle: Overview and challanges, in: Nitrogen in Marine Environment, edited by: Capone, D. G., Bronk, D. A., Mulholland, M. R., and Carpenter, E. J., Elsevier Inc., 1–51, 2008.

Gruber, N. and Sarmiento, J. L.: Global patterns of marine nitrogen fixation and denitrification, Global Biogeochem. Cy., 11, 235–266, doi:10.1029/97GB00077, 1997.

Hamersley, M. R., Lavik, G., Woebken, D., Rattray, J. E., Lam, P., Hopmans, E. C., Damste, J. S. S., Kruger, S., Graco, M., Gutierrez, D., and Kuypers, M. M. M.: Anaerobic ammonium oxidation in the Peruvian oxygen minimum zone, Limnol. Oceanogr., 52, 923–933, doi:10.4319/lo.2007.52.3.0923, 2007.

Kalvelage, T., Jensen, M. M., Contreras, S., Revsbech, N. P., Lam, P., Günter, M., LaRoche, J., Lavik, G., and Kuypers, M. M. M.: Oxygen sensitivity of anammox and coupled N-cycle processes in oxygen minimum zones, PLoS One TS3, 6, e29299, doi:10.1371/journal.pone.0029299, 2011.

Kuypers, M. M. M., Sliekers, A. O., Lavik, G., Schmid, M., Jorgensen, B. B., Kuenen, J. G., Damste, J. S. S., Strous, M., and Jetten, M. S. M.: Anaerobic ammonium oxidation by anammox bacteria in the Black Sea, Nature, 422, 608–611, doi:10.1038/nature01472, 2003.

Lam, P., Lavik, G., Jensen, M. M., van de Vossenberg, J., Schmid, M., Woebken, D., Dimitri, G., Amann, R., Jetten, M. S. M., and Kuypers, M. M. M.: Revising the nitrogen cycle in the Peruvian oxygen minimum zone, P. Acad. Sci. USA, 106, 4752–4757, doi:10.1073/pnas.0812444106, 2009.

McGillicuddy, D. J. and Robinson, A. R.: Eddy-induced nutrient supply and new production in the Sargasso Sea, Deep-Sea Res. Pt. 1, 44, 1427–1450, doi:10.1016/S0967-0637(97)00024-1, 1997.

McGillicuddy, D. J., Robinson, A. R., Siegel, D. A., Jannasch, H. W., Johnson, R., Dickeys, T., McNeil, J., Michaels, A. F., and Knap, A. H.: Influence of mesoscale eddies on new production in the Sargasso Sea, Nature, 394, 263–266, doi:10.1038/28367, 1998.

McIlvin, M. R. and Altabet, M. A.: Chemical conversion of nitrate and nitrite to nitrous oxide for nitrogen and oxygen isotopic analysis in freshwater and seawater, Anal. Chem., 77, 5589–5595, doi:10.1021/ac050528s, 2005.

Naqvi, S. W. A., Jayakumar, D. A., Narvekar, P. V., Naik, H., Sarma, V., D'Souza, W., Joseph, S., and George, M. D.: Increased marine production of N_2O due to intensifying anoxia on the Indian continental shelf, Nature, 408, 346–349, doi:10.1038/35042551, 2000.

Redfield, A. C.: The biological control of chemical factors in the environment, Am. Sci., 46, 205–221, 1958.

Richards, F. A.: Anoxic basins and fjords, in: Chemical Oceanography, edited by: Riley, J. P. and Skirrow, G., Academic Press, London, 611–643, 1965.

Ryabenko, E., Altabet, M. A., and Wallace, D. W. R.: Effect of chloride on the chemical conversion of nitrate to nitrous oxide for $\delta^1$5N analysis, Limnol. Oceanogr. Methods, 7, 545–552, 2009.

Ryabenko, E., Kock, A., Bange, H. W., Altabet, M. A., and Wallace, D. W. R.: Contrasting biogeochemistry of nitrogen in the Atlantic and Pacific oxygen minimum zones, Biogeosciences 9, 203–215, 10.5194/bg-9-203-2012, 2012.

Sigman, D. M., Granger, J., DiFiore, P. J., Lehmann, M. M., Ho, R., Cane, G., and van Geen, A.: Coupled nitrogen and oxygen isotope measurements of nitrate along the eastern North Pacific margin, Global Biogeochem. Cy., 19, GB4022, doi:10.1029/2005GB002458, 2005.

Sigman, D. M., DiFiore, P. J., Hain, M. P., Deutsch, C., Wang, Y., Karl, D. M., Knapp, A. N., Lehmann, M. F., and Pantoja, S.: The dual isotopes of deep nitrate as a constraint on the cycle and budget of oceanic fixed nitrogen, Deep-Sea Res. Pt. 1, 56, 1419–1439, doi:10.1016/j.dsr.2009.04.007, 2009.

Stramma, L., Johnson, G. C., Sprintall, J., and Mohrholz, V.: Expanding oxygen-minimum zones in the tropical oceans, Science, 320, 655–658, doi:10.1126/science.1153847, 2008

Stramma, L., Visbeck, M., Brandt, P., Tanhua, T., and Wallace, D.: Deoxygenation in the oxygen minimum zone of the eastern tropical North Atlantic, Geophys. Res. Lett., 36, L20607, doi:10.1029/2009gl039593, 2009.

Strub, P. T., Allen, J. S., Huyer, A., and Smith, G. J.: Seasonal cycles of currents, temperatures, winds, and sea level over the northeast Pacific continental shelf: 35° to 48° N, J. Geophys. Res., 92, 1507–1526, doi:10.1029/JC092iC02p01507, 1987. TS4

Thamdrup, B., Dalsgaard, T., Jensen, M. M., Ulloa, O., Farias, L., and Escribano, R.: Anaerobic ammonium oxidation in the oxygen-deficient waters off northern Chile, Limnol. Oceanogr., 51, 2145–2156, doi:10.4319/lo.2006.51.5.2145, 2006.

Voss, M. and Montoya, J. P.: Nitrogen cycle. Oceans apart, Nature, 461, 49–50, doi:10.1038/461049a, 2009.

Voss, M., Dippner, J. W., and Montoya, J. P.: Nitrogen isotope patterns in the oxygen-deficient waters of the Eastern Tropical North Pacific Ocean, Deep-Sea Res. Pt. 1, 48, 1905–1921, doi:10.1016/S0967-0637(00)00110-2, 2001.

Ward, B. B., Devol, A. H., Rich, J. J., Chang, B. X., Bulow, S. E., Naik, H., Pratihary, A., and Jayakumar, A.: Denitrification as the dominant nitrogen loss process in the Arabian Sea, Nature, 461, 78–81, doi:10.1038/nature08276, 2009.

Ward, B. B., Tuit, C. B., Jayakumar, A., Rich, J. J., Moffett, J., and Naqvi, S. W. A.: Organic carbon, and not copper, controls denitrification in oxygen minimum zones of the ocean, Deep-Sea Res. Pt. 1, 55, 1672–1683, 2008.

Remarks from the Typesetter

TS1 reference is missing in reference list
TS2 please provide pages
TS3 please provide correct journal name
TS4 please provide article number